SUPPLEMENTAL FIGURES

Figure S1, Related to Figure 1. Selective Production of L-2HG in Response to Hypoxia. (A and B) The absolute concentration of 2HG in hypoxic SF188 cells is 304 +/- 81 μM (mean +/- SD from 3 independent experiments). The (A) standard curve and (B) calculations are shown for one of the experiments used to quantitate intracellular 2HG concentration in hypoxic SF188 cells (see Experimental Procedures for details). (C and D) HEK293T cells were transfected with (C) siRNAs targeting D2HGDH (D2HGDH-a, -b) or L2HGDH (L2HGDH-a, -b) or (D) empty vector (Vector) or vector encoding D2HGDH or L2HGDH. 48 hr after transfection, cells were transferred to 21% or 0.5% O_2 for an additional 24 hr, followed by measurement of intracellular 2HG. Western blot confirms target knockdown efficiency with expression of either α-tubulin or S6 protein shown as loading controls. For each panel, representative data from 1 of ≥2 independent experiments are shown. (E) Schematic showing L-2-hydroxyglutarate (blue) after sequential derivatization with R(-)-2-butanol (green) and acetic anhydride (red) (see Experimental Procedures for details). (F) Representative mass spectra used to identify R(-)-2-butanol/acetic anhydride-derivatized 2HG enantiomers (*m/z* 173 plus confirmatory ions 187, 229, and 260). The structure of the *m/z* 173 species is shown. (G and H) Metabolites from (G) HEK293T cells or (H) SV40-immortalized MEFs cultured in normoxia (21% O_2) or hypoxia (0.5% O_2) were subjected to chiral derivatization as in (E and F) to allow separation of 2HG enantiomers by GC-MS. L-2HG (left) elutes at a shorter retention time than D-2HG (right) as in demonstrated in Figure 1D. Representative data from 1 of ≥2 independent experiments are shown.

Figure S2, Related to Figure 3. Confirming Enzymatic Sources and Dependencies of Hypoxia-Induced L-2HG. (A, B, C) HEK293T cells were transfected with siRNAs targeting (A)

IDH1 (IDH1-a, -b) and/or IDH2 (IDH2-a, -b), (B) LDHA (LDHA-a, -b, -c, -d), or (C) both LDHA (LDHA-b, -d) and MDH2 (MDH2-a, -b). (D, E, F) SF188 cells were transfected with siRNAs targeting (D) LDHB (LDHB-a, -b, -c, -d) or (E and F) HIF1α (HIF1α-a, -b, -c). (G) HEK293T cell were transfected with siRNAs targeting HIF1α (HIF1α-a, -b, -c). For (A, B, C, D, E, F, G), 48 hr after transfection, cells were transferred to 21% or 0.5% O_2 for an additional 24 to 48hr, followed by measurement of intracellular 2HG. (H) VHL-deficient RCC4 cells with stable expression of a non-targeting shRNA (Cont) or shRNA targeting HIF1α (HIF1α) were cultured for 48 hr in 21% or 0.5% O_2 followed by measurement of intracellular 2HG. Western blot confirms target knockdown efficiency with expression of either S6 protein or α-tubulin shown as loading controls. For each panel, representative data from 1 of ≥2 independent experiments are shown.

Figure S3, Related to Figure 3. Structural Modeling Shows that the Active Site of LDHA can Sterically Accommodate Binding of α-KG in a Geometry Amenable for Reduction to L-2HG. (A and C) Docked poses of pyruvate and α-KG to the active site of LDHA with NADH. (B and D) Docked poses of L-lactate and L-2HG to the active site of LDHA with NAD+. The shadowed cloud is a representation of predicted empty space within the substrate-binding pocket. Predicted hydrogen bonds are shown in blue. Residues shown as lines are Arg168 (chartreuse), Thr247 (orange), His192 (yellow), Arg105 (purple), Asn137 (green), and Gln99 (blue). Docking utilized PDB accession code 1I10 (Read et al., 2001). The red boxes highlight the spatial configurations of the carboxylic acid head group and adjacent carbonyl group of each substrate in relation to the hydride group of NADH, which constrains the reductive reactions to produce the L-(S)- enantiomers of the corresponding α-hydroxyl acids.

Figure S4, Related to Figure 4. Enhanced Trimethylation of Histone 3 Lysine 9 in Hypoxic Glioblastoma Tumors. (A, C, E) HIF1α and (B, D, F) H3K9me3 expression from the set of 47

human glioblastoma core biopsy specimens. Each row represents an individual patient with sections stained for the indicated markers. The asterisks in (E and F) indicate a region of necrosis. Scale bars are shown in the bottom left corner of each image. (G) SF188 glioblastoma cells stably infected with empty lentiviral vector (Vector) or lentiviral vector encoding L2HGDH were cultured for 48 hr in 21% or 0.5% O_2, followed by measurement of intracellular 2HG. Western blots confirm overexpression of L2HGDH and hypoxia-induced expression of HIF1α. S6 protein is shown as a loading control. For (G), representative data from 1 of 3 independent experiments are shown.

Figure S1

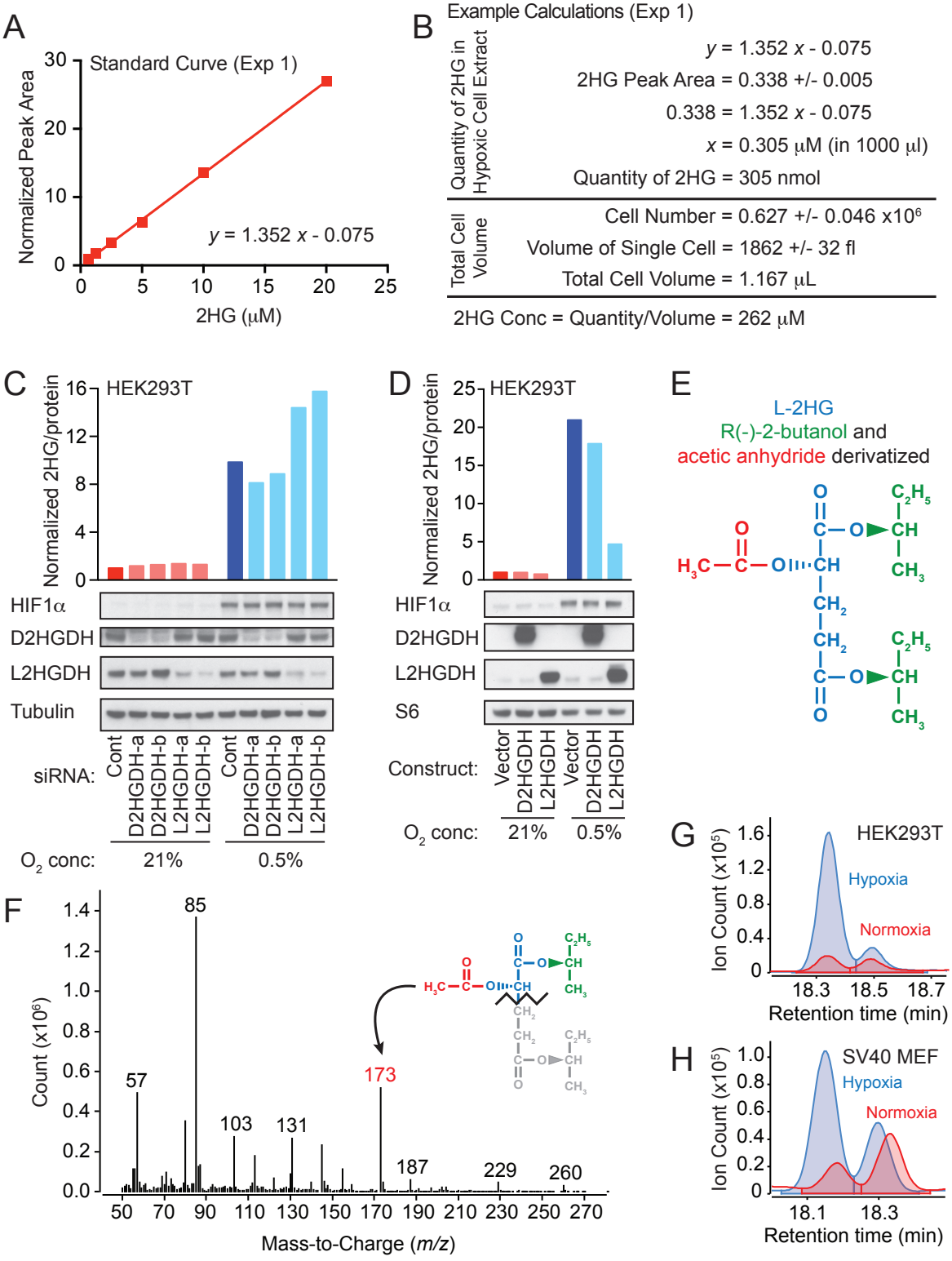
A
Standard Curve (Exp 1)
Normalized Peak Area
y = 1.352 x - 0.075
2HG (μM)
B
Example Calculations (Exp 1)
Quantity of 2HG in Hypoxic Cell Extract
y = 1.352 x - 0.075
2HG Peak Area = 0.338 +/- 0.005
0.338 = 1.352 x - 0.075
x = 0.305 μM (in 1000 μl)
Quantity of 2HG = 305 nmol
Total Cell Volume
Cell Number = 0.627 +/- 0.046 x10^6
Volume of Single Cell = 1862 +/- 32 fl
Total Cell Volume = 1.167 μL
2HG Conc = Quantity/Volume = 262 μM
C
HEK293T
Normalized 2HG/protein
HIF1α
D2HGDH
L2HGDH
Tubulin
siRNA:
Cont
D2HGDH-a
D2HGDH-b
L2HGDH-a
L2HGDH-b
O2 conc:
21%
0.5%
D
HEK293T
Normalized 2HG/protein
HIF1α
D2HGDH
L2HGDH
S6
Construct:
Vector
D2HGDH
L2HGDH
O2 conc:
21%
0.5%
E
L-2HG
R(-)-2-butanol and
acetic anhydride derivatized
F
Count (x10^6)
85
57
103
131
173
187
229
260
Mass-to-Charge (m/z)
G
HEK293T
Hypoxia
Normoxia
Ion Count (x10^5)
Retention time (min)
H
SV40 MEF
Hypoxia
Normoxia
Ion Count (x10^5)
Retention time (min)

Figure S2

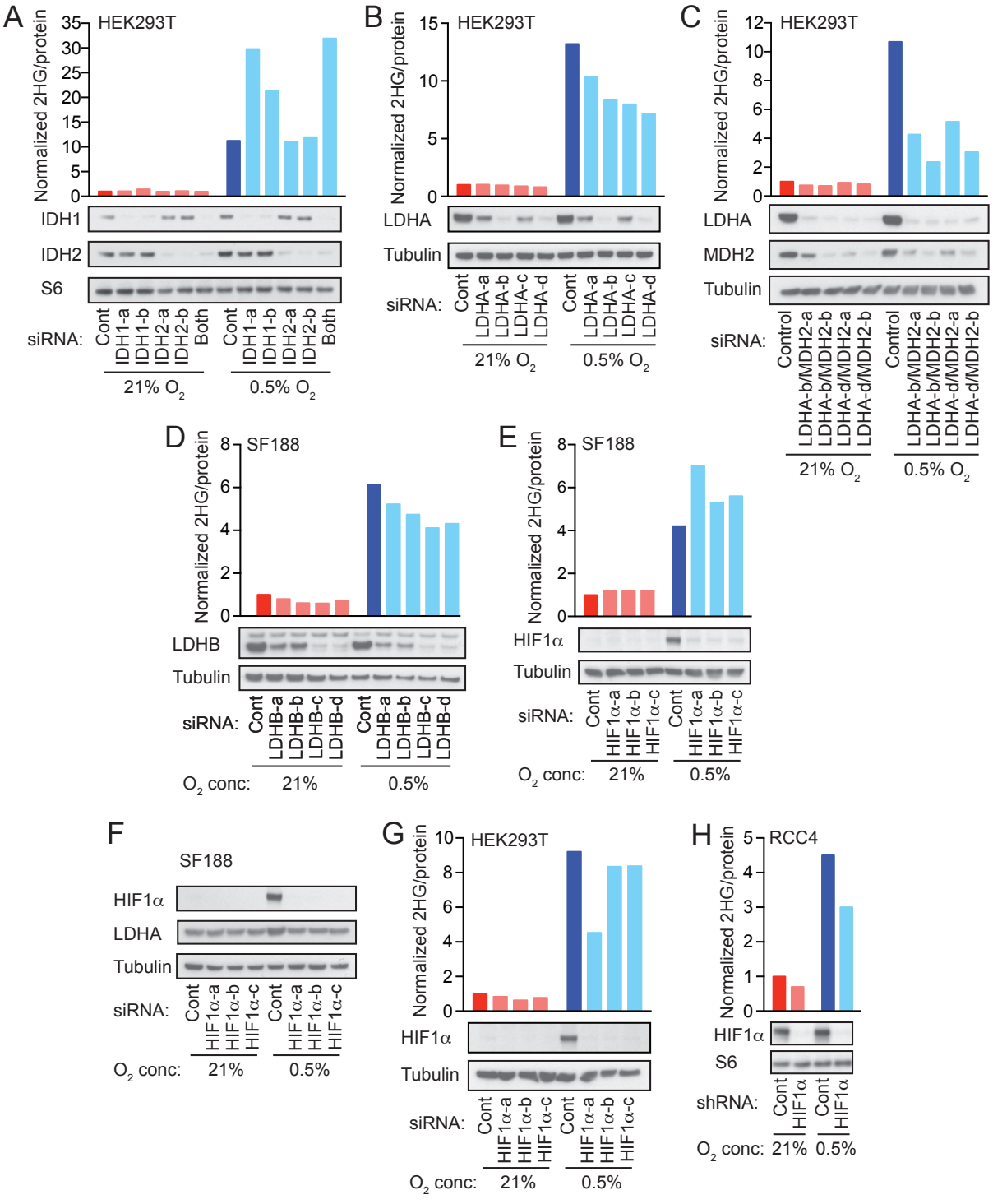
A
HEK293T
Normalized 2HG/protein
IDH1
IDH2
S6
siRNA:
Cont
IDH1-a
IDH1-b
IDH2-a
IDH2-b
Both
21% O2
0.5% O2
B
HEK293T
LDHA
Tubulin
LDHA-a
LDHA-b
LDHA-c
LDHA-d
C
HEK293T
MDH2
Control
LDHA-b/MDH2-a
LDHA-b/MDH2-b
LDHA-d/MDH2-a
LDHA-d/MDH2-b
D
SF188
LDHB
LDHB-a
LDHB-b
LDHB-c
LDHB-d
O2 conc:
21%
0.5%
E
SF188
HIF1α
HIF1α-a
HIF1α-b
HIF1α-c
F
SF188
G
HEK293T
H
RCC4
shRNA:

Figure S3

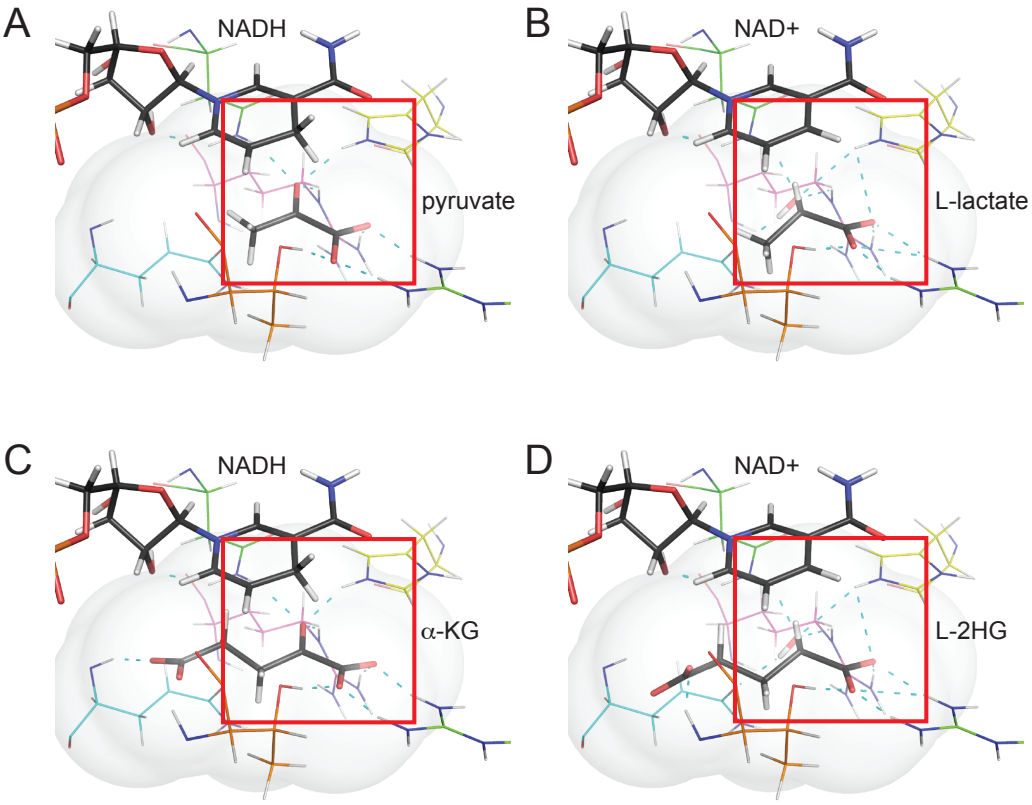

Figure S4

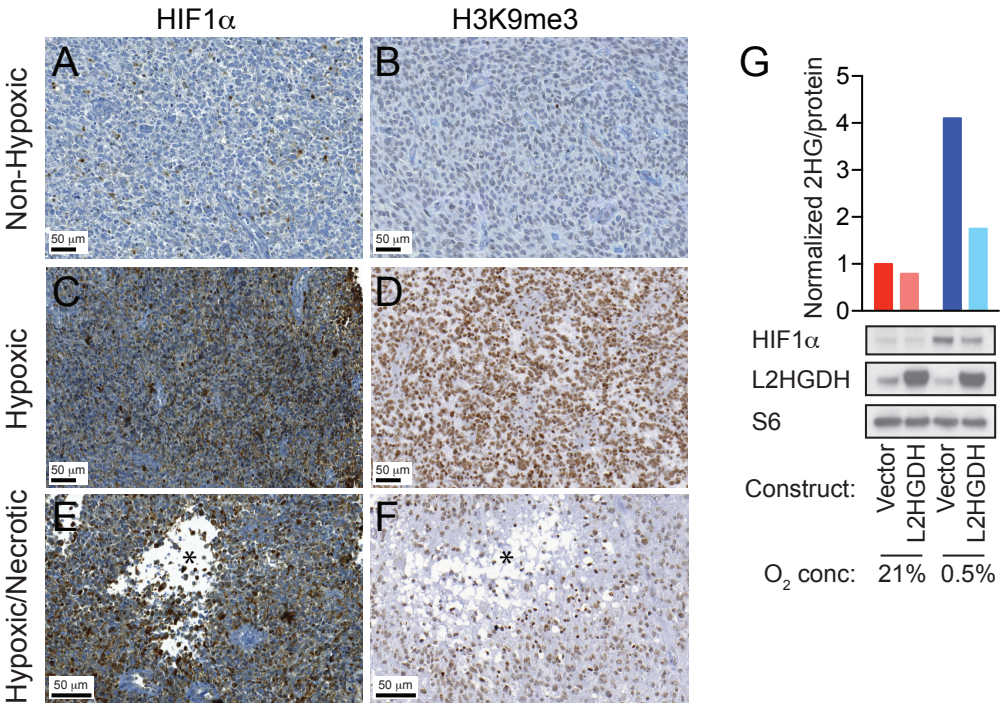
HIF1α
H3K9me3
Non-Hypoxic
Hypoxic
Hypoxic/Necrotic
A
B
C
D
E
F
50 μm
*
G
Normalized 2HG/protein
0
1
2
3
4
5
HIF1α
L2HGDH
S6
Construct:
Vector
L2HGDH
Vector
L2HGDH
O2 conc:
21%
0.5%

SUPPLEMENTAL EXPERIMENTAL PROCEDURES

siRNA and shRNA Experiments

For siRNA experiments, SF188 or HEK293T cells were reverse-transfected with siRNA mixed with Lipofectamine RNAiMAX (Life Technologies) in Opti-MEM® Reduced Serum Medium (Life Technologies) as described by the manufacturer at 30 nM final concentration. D2HGDH or L2HGDH cDNAs were cloned by standard methods into the pCDNA3.1 (Addgene) or pCDH-CMV-MCS-EF1-Puro vector (pCDH) (System Biosciences). For overexpression experiments, HEK293T cells were transfected with D2HGDH or L2HGDH pCDNA3.1 vectors (2 μg) mixed with FuGENE 6 Transfection Reagent (Promega). For generating SF188 cell lines with stable expression of shRNAs (PLKO.1), empty vector (pCDH), or L2HGDH (pCDH), supernatant from 293T cells transfected with helper virus and plasmids was collected after 72 hr, filtered and applied to SF188 parental cells overnight. Puromycin-resistant cells were selected by continuous culture puromycin 1 μg/ml.

The following TRC version 1 shRNAs in PLKO.1 vector (Sigma) were used:

shL2HGDH-1 (L1) = clone ID: NM_024884.1-1113s1c1, sequence: CCGGCCACAGATGTTATGGATATAACTCGAGTTATATCCATAACATCTGTGGTTTTTG;

shL2HGDH-2 (L2) = clone ID: NM_024884.1-1370s1c1, sequence: CCGGCGCATTCTTCATGTGAGAAATCTCGAGATTTCTCACATGAAGAATGCGTTTTTG;

shL2HGDH-3 (L3) = clone ID: NM_024884.1-1217s1c1, sequence: CCGGGCAACAGTGAAGTATCTTCAACTCGAGTTGAAGATACTTCACTGTTGCTTTTTG;

shL2GHDH-4 (L4) = clone ID: NM_024884.1-674s1c1, sequence: CCGGGCTTTGTCATTTGCCCAGGATCTCGAGATCCTGGGCAAATGACAAAGCTTTTTG;

shD2HGDH-2 (D2) = clone ID: NM_152783.2-630s1c1, sequence: CCGGGCGTGTCTGGAATTCTGGTTTCTCGAGAAACCAGAATTCCAGACACGCTTTTTG;

shD2HGDH-3 (D3) = clone ID: NM_152783.2-1270s1c1, sequence:

CCGGCGACCAGAGGAAAGTCAAGATCTCGAGATCTTGACTTTCCTCTGGTCGTTTTTG;

shD2HGDH-4 (D4) = clone ID: NM_152783.2-319s1c1, sequence:

CCGGGCCGTTCTCCACGGTGTCTAACTCGAGTTAGACACCGTGGAGAACGGCTTTTTG;

shD2HGDH-5 (D5) = clone ID: NM_152783.2-1066s1c1, sequence:

CCGGCCTGTCTGCATTCGAGTTCATCTCGAGATGAACTCGAATGCAGACAGGTTTTTG.

The following siRNAs from Thermo Scientific were used:

siIDH1-a = J-008294-10, target sequence: GCAUAAUGUUGGCGUCAAA;

siIDH1-b = J-008294-11, target sequence: GCUUGUGAGUGGAUGGGUA;

siIDH2-a = J-004013-09, target sequence: GCAAGAACUAUGACGGAGA;

siIDH2-b = J-004013-12, target sequence: GCGCCACUAUGCCGACAAA;

siMDH1-a = J-009264-10, target sequence: GGGAGAAUUUGUCACGACU;

siMDH1-b = J-009264-12, target sequence: AGGUUAUUGUUGUGGGUAA;

siMDH2-a = J-008439-10, target sequence: GAUCUGAGCCACAUCGAGA;

siMDH2-b = J-008439-12, target sequence: CGCCUGACCCUCUAUGAUA;

siLDHA-a = J-008201-05, target sequence: GGAGAAAGCCGUCUUAAUU;

siLDHA-b = J-008201-06, target sequence: GGCAAAGACUAUAAUGUAA;

siLDHA-c = J-008201-07, target sequence: UAAGGGUCUUUACGGAAUA;

siLDHA-d = J-008201-08, target sequence: AAAGUCUUCUGAUGUCAUA;

siLDHB-a = J-009779-05, target sequence: CAACUGGGCUAUUGGAUUA;

siLDHB-b = J-009779-06, target sequence: UGGCUGAUCUUAUUGAAUC;

siLDHB-c = J-009779-07, target sequence: UCAUCAAGCUAAAAGGAUA;

siLDHB-d = J-009779-08, target sequence: GUACAGUCCUGAUUGCAUC.

The following siRNAs from Ambion were used:

siHIF1α-a = s6539, sense sequence: CCAUAUAGAGAUACUCAAAtt;

siHIF1α-b = s6540, sense sequence: CCGAAUUGAUGGGAUAUGAtt;

siHIF1α-c = s6541, sense sequence: CCUCAGUGUGGGUAUAAGAtt.

Western Blotting

Cell lysates were extracted in 1x RIPA buffer (Cell Signaling), sonicated, centrifuged at 14,000*g* at 4ºC, and supernatants were collected. For histone acid-extraction, cells were lysed in hypotonic lysis buffer (Amresco) for 1 hr. H_2SO_4 was added to 0.2 N overnight at 4^{o}C with rotation, and supernatants were collected after centrifugation. Histones were precipitated in 33% TCA, washed with acetone, and resuspended in deionized water. Cleared cell lysates or histone preparations were normalized for total protein concentration. Samples were separated by SDS-PAGE, transferred to nitrocellulose membranes (Life Technologies), blocked in 5% milk prepared in Tris buffered saline with 0.1% Tween 20 (TBST), incubated with primary antibodies overnight at 4^{o}C then horseradish peroxidase (HRP)-conjugated secondary antibodies (GE Healthcare, NA931V and NA934V) for 1 hr the following day. After ECL application (Thermo Scientific), imaging was performed using the SRX-101A (Konica Minolta). For *in vitro* histone demethylase assays, bulk calf thymus histones (Sigma) were incubated with GST-tagged KDM4C (BPS Bioscience) in a reaction mixture containing Tris-HCl 50 mM, pH 8.0, protease inhibitors, α-KG 1 mM, FeSO4 100 micromolar, and ascorbic acid 2 micromolar. The reaction mixture was incubated at 37°C for 4 hr in the absence or presence of various concentrations of L-2HG or D-2HG (Sigma). H3K9me3 levels were analyzed by Western blot with total histone H3 used as the loading control. Primary antibodies used included: anti-L2HGDH (Proteintech, 15707-1-AP), anti-D2HGDH (Proteintech, 13895-1-AP), anti-LDHA (Cell Signaling, 2012), anti-IDH1 (anti-IDH2 (Abcam, ab55271), anti-MDH1 (Abcam, ab55528), anti-MDH2 (Abcam, ab96193), anti-tubulin (Sigma, T9026), anti-S6 ribosomal protein (Cell Signaling, 2317), anti-HIF1α (BD Biosciences, 610959), anti-H3 (Cell Signaling, 4499), and anti-H3K9me3 (Active Motif, 39765).

Metabolite Extraction and GC-MS Analysis

Metabolites were extracted with 1 mL ice-cold 80% methanol supplemented with 2 micromolar deuterated 2-hydroxyglutarate (D-2-hydroxyglutaric-2,3,3,4,4-d_5 acid; deuterated-D-2HG) as an internal standard. After overnight incubation at -80°C, lysates were harvested, sonicated, then centrifuged at 21,000*g* for 20 minutes at 4°C to remove protein. Extracts were dried in an evaporator (Genevac EZ-2 Elite) and resuspended by incubation at 30°C for 90 min in 50 microliters of methoxyamine hydrochloride 40 mg/mL in pyridine. Metabolites were further derivatized by addition of 80 microliters of MSTFA + 1% TCMS (Thermo Scientific) and 70 microliters of ethyl acetate (Sigma) and incubated at 37°C for 30 min. Samples were analyzed using an Agilent 7890A GC coupled to Agilent 5975C mass selective detector. The GC was operated in splitless mode with constant helium gas flow at 1 mL/min. 1 μL of derivatized metabolites was injected onto an HP-5MS column and the GC oven temperature ramped from 60°C to 290°C over 25 minutes. Peaks representing compounds of interest were extracted and integrated using MassHunter software (Agilent Technologies) and then normalized to both the internal standard (deuterated-D-2HG) peak area and protein content. Ions used for quantification of metabolite levels were 2HG *m/z* 247 and deuterated-2HG *m/z* 252. Peaks were manually inspected and verified relative to known spectra for each metabolite. To construct the standard curve for quantitation of intracellular 2HG levels, 1 ml volumes of metabolite extracts were spiked with defined concentrations of L-(S)-2HG standard (Sigma), then processed and analyzed as above. The standard curve calculations were performed using Prism. Cell counts and volumes of triplicate wells were determined with a Beckman Coulter Counter. For isotope tracing studies, media was changed at the indicated time before harvest using glucose- and glutamine-free DMEM media supplemented with ^{12}C-glucose (Sigma) and ^{12}C-glutamine (Gibco) or the ^{13}C versions of each metabolite, [U-^{13}C]glucose or [U-^{13}C]glutamine (Cambridge Isotope Labs). Samples were harvested in 80% methanol without internal standard. Enrichment of ^{13}C

was assessed by quantifying the abundance of the 2HG ions, *m/z* 349-362. Correction for natural isotope abundance was performed using IsoCor software (Millard et al., 2012).

Molecular Docking of Putative LDHA Substrates

Docking of putative substrate and product molecules was performed using Glide in Maestro 2014-3 (Friesner et al., 2004; Friesner et al., 2006; Halgren et al., 2004; Schrödinger, 2014). Ligands were docked into chain A of PDB structure 1I10 after removing crystallographic waters and ligands except for NADH (Read et al., 2001). Missing side chains and loops were automatically rebuilt using Prime (Jacobson et al., 2002; Jacobson et al., 2004). PROPKA was used to assign protonation states compatible with a pH of 7 (Olsson et al., 2011; Sondergaard et al., 2011). Bond orders for NADH or NAD+ were manually verified to avoid misassignment by PROPKA. Restrained minimization was performed using OPLS2005 (Banks et al., 2005). Oxamate was used as a reference ligand to define the binding site, after adding fictitious atoms to ensure minimum atom requirement for binding site definition was met. Hydroxyl and thiol groups were allowed to rotate during grid generation. Pyruvate and α-ketoglutarate were docked in the presence of crystallographic NADH. Lactate and L-2-hydroxyglutarate were docked in the presence of NAD+ modeled from crystallographic NADH by alteration of bond orders. Carboxylic acid moieties of the ligands were fully deprotonated. Docking was performed using Extra Precision Glide with flexible ligands (Friesner et al., 2004; Friesner et al., 2006; Halgren et al., 2004). Docking poses were minimized post-docking. The resulting conformations were clustered within a 1 angstrom RMSD cutoff. This resulted in a single representative pose for each of the docked ligands. All steps utilized default parameters unless otherwise noted. Poses and predicted hydrogen bonds were visualized using PyMOL (The PyMOL Molecular Graphics System, Version 1.7.0.0 Schrödinger, LLC).

Human Glioblastoma Specimens and Immunohistochemical Analysis

Immunohistochemical studies and quantification were performed as previously described (Venneti et al., 2013). In brief, immunostaining was performed using the Discovery XT processor (Ventana Medical Systems). Tissue sections were blocked for 30 min in 10% normal goat serum in 2% BSA in PBS. Sections were incubated for 5 hr with 10 microgram/ml of the mouse monoclonal anti-HIF1α (Alexis Biochem, ALX-210-069) or 0.1 microgram/ml of the rabbit polyclonal anti-H3K9me3 antibodies (Abcam, ab8898). Tissue sections were then incubated for 60 min with biotinylated goat anti-mouse or anti-rabbit IgG (Vector labs, PK6102 and PK6101) at 1:200 dilution. Blocker D, Streptavidin-HRP and DAB detection kit (Ventana Medical Systems) were used according to the manufacturer instructions.

For automated scoring, slides were scanned using a Pannoramic Flash 250 scanner (Perkin Elmer, Waltham MA) and viewed through the Pannoramic viewer software program (3D Histech, Waltham MA). An individual blinded to the experimental design captured JPEG images at 10X magnification. Quantification of immunostaining on each JPEG was conducted using an automated analysis program with Matlab's image processing toolbox based on previously described methodology (Venneti et al., 2013). The algorithm used color segmentation with RGB color differentiation, K-Means Clustering and background-foreground separation with Otsu's thresholding. To arrive at a score the number of extracted pixels were multiplied by their average intensity for each core (represented as pixel units). The final score for a given case and marker was calculated by averaging the score of two cores (for each case) for a given marker.

SUPPLEMENTAL REFERENCES

Banks, J.L., Beard, H.S., Cao, Y., Cho, A.E., Damm, W., Farid, R., Felts, A.K., Halgren, T.A., Mainz, D.T., Maple, J.R.*, et al.* (2005). Integrated Modeling Program, Applied Chemical Theory (IMPACT). Journal of Computational Chemistry *26*, 1752-1780.

Friesner, R.A., Banks, J.L., Murphy, R.B., Halgren, T.A., Klicic, J.J., Mainz, D.T., Repasky, M.P., Knoll, E.H., Shelley, M., Perry, J.K.*, et al.* (2004). Glide: a new approach for rapid, accurate docking and scoring. 1. Method and assessment of docking accuracy. Journal of Medicinal Chemistry *47*, 1739-1749.

Friesner, R.A., Murphy, R.B., Repasky, M.P., Frye, L.L., Greenwood, J.R., Halgren, T.A., Sanschagrin, P.C., and Mainz, D.T. (2006). Extra precision glide: docking and scoring incorporating a model of hydrophobic enclosure for protein-ligand complexes. Journal of Medicinal Chemistry *49*, 6177-6196.

Halgren, T.A., Murphy, R.B., Friesner, R.A., Beard, H.S., Frye, L.L., Pollard, W.T., and Banks, J.L. (2004). Glide: a new approach for rapid, accurate docking and scoring. 2. Enrichment factors in database screening. Journal of Medicinal Chemistry *47*, 1750-1759.

Jacobson, M.P., Friesner, R.A., Xiang, Z., and Honig, B. (2002). On the role of the crystal environment in determining protein side-chain conformations. Journal of Molecular Biology *320*, 597-608.

Jacobson, M.P., Pincus, D.L., Rapp, C.S., Day, T.J., Honig, B., Shaw, D.E., and Friesner, R.A. (2004). A hierarchical approach to all-atom protein loop prediction. Proteins *55*, 351-367.

Millard, P., Letisse, F., Sokol, S., and Portais, J.C. (2012). IsoCor: correcting MS data in isotope labeling experiments. Bioinformatics *28*, 1294-1296.

Olsson, M.H.M., Sondergaard, C.R., Rostkowski, M., and Jensen, J.H. (2011). PROPKA3: Consistent Treatment of Internal and Surface Residues in Empirical pK(a) Predictions. J Chem Theory Comput *7*, 525-537.

Read, J.A., Winter, V.J., Eszes, C.M., Sessions, R.B., and Brady, R.L. (2001). Structural basis for altered activity of M- and H-isozyme forms of human lactate dehydrogenase. Proteins *43*, 175-185.

Schrödinger (2014). Schrödinger Release 2014-3: Maestro, version 9.9, Schrödinger, LLC, New York, NY.

Sondergaard, C.R., Olsson, M.H.M., Rostkowski, M., and Jensen, J.H. (2011). Improved Treatment of Ligands and Coupling Effects in Empirical Calculation and Rationalization of pK(a) Values. J Chem Theory Comput *7*, 2284-2295.

Venneti, S., Garimella, M.T., Sullivan, L.M., Martinez, D., Huse, J.T., Heguy, A., Santi, M., Thompson, C.B., and Judkins, A.R. (2013). Evaluation of histone 3 lysine 27 trimethylation (H3K27me3) and enhancer of Zest 2 (EZH2) in pediatric glial and glioneuronal tumors shows decreased H3K27me3 in H3F3A K27M mutant glioblastomas. Brain Pathol *23*, 558-564.